Journal Pre-proofs

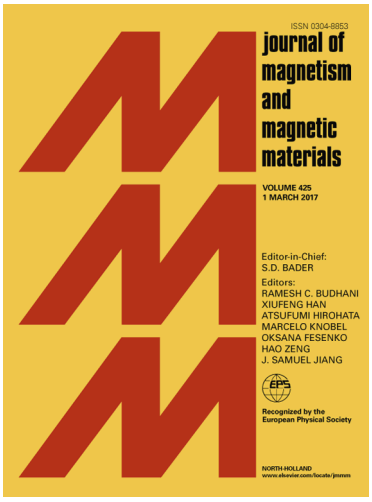

Novel room-temperature ferromagnetism in Gd-doped 2-dimensional $Ti_3C_2T_x$ MXene semiconductor for spintronics

Sunaina Rafiq, SaifUllah Awan, Ren-Kui Zheng, Zhenchao Wen, Malika Rani, Deji Akinwande, Syed Rizwan

PII: S0304-8853(19)32540-5
DOI: https://doi.org/10.1016/j.jmmm.2019.165954
Reference: MAGMA 165954

To appear in: *Journal of Magnetism and Magnetic Materials*

Received Date: 23 July 2019
Revised Date: 11 September 2019
Accepted Date: 4 October 2019

Please cite this article as: S. Rafiq, S. Awan, R-K. Zheng, Z. Wen, M. Rani, D. Akinwande, S. Rizwan, Novel room-temperature ferromagnetism in Gd-doped 2-dimensional $Ti_3C_2T_x$ MXene semiconductor for spintronics, *Journal of Magnetism and Magnetic Materials* (2019), doi: https://doi.org/10.1016/j.jmmm.2019.165954

Novel room-temperature ferromagnetism in Gd-doped 2-dimensional $Ti_3C_2T_x$ MXene semiconductor for spintronics

Sunaina Rafiq,[a,b] SaifUllah Awan,[c] Ren-Kui Zheng,[d] Zhenchao Wen,[e] Malika Rani,[b1)] Deji Akinwande,[f] Syed Rizwan,[a1)]

[a]*Physics Characterization and Simulations Lab, School of Natural Sciences (SNS), National University of Sciences and Technology (NUST), Islamabad 54000, Pakistan.*

[b]*Department of Physics, The Women University Multan, Multan 66000, Pakistan.*

[c]*Department of Electrical Engineering, NUST College of Electrical and Mechanical Engineering, National University of Sciences and Technology (NUST), Islamabad 54000, Pakistan.*

[d]*State Key Laboratory of High Performance Ceramics and Superfine Microstructure, Shanghai Institute of Ceramics, Chinese Academy of Sciences, Shanghai 200050, China.*

[e]*National Institute for Materials Science (NIMS), Tsukuba, Ibaraki 305-0047, Japan.*

[f]*Microelectronics Research Center, The University of Texas at Austin, Austin, Texas 78758, United States*

ABSTRACT

Two-dimensional nanosheets of MXene (Ti_3C_2) and Gd^{+3}-doped MXene (Ti_3C_2) have been synthesized superficially by using the cost-effective co-precipitation method. The hexagonal crystal structure doped by Gd was confirmed using X-ray Diffraction. The doping was further confirmed by using scanning electron microscopy, energy dispersive X-ray spectroscopy and Fourier transformed infra-red spectroscopy. Furthermore, UV-Vis spectroscopy absorption spectra, followed by a Tauc-plot, revealed a band-gap value of 1.93eV for Gd-doped MXene, reduced from that for pure MXene (2.06eV). The magnetic measurement of undoped and doped MXene indicate a clear ferromagnetic hysteresis existing at room-temperature. The asymmetric spatial spin-density of states (s-DOS) for undoped MXene is attributed to the existence of spin-up and spin-down electrons of Ti-3d atoms at top and bottom Titanium layers. The strength of one of the spin-type (spin-up) increases more than two-folds at room-temperature after the doping of Gd^{+3} cations due to the fact that it contains more unpaired electrons around Fermi level making the MXene more ferromagnetic. The present report establishes the existence of ferromagnetism introduced by doping of Gd^{+3} cation in Ti_3C_2 MXene at room-temperature making it a suitable candidate for two-dimensional spintronic devices operating at room-temperature.

Keywords: Gadolinium, Ti_3C_2-MXene, Ferromagnetism, Spintronics

[1] Electronic mail: syedrizwan@sns.nust.edu.pk, dr.malikarani@yahoo.com.

INTRODUCTION

Two-dimensional (2D) ferromagnetic nano-materials have been vigorously pursued for spintronics since the discovery of graphene, as their spin-dependent transport applications are very important for nanoscale data storage memory devices[1] [2]. Many researchers focused on 2D ferromagnetic nanoscale materials, mainly the graphene and transition metal dichalcogenides (TMDs). Ferromagnetism is experimentally observed in 2D materials containing graphene with point defects/vacancies [3] [4], stretched graphene nanobubbles [5], and zig-zag corners at the grain boundaries of TMD nanosheets [6] in which the proposed origin of ferromagnetism is due to unsaturated p-orbitals. However, these 2D systems suffer from severe complications such as poor charge carrier concentration and the deficiency of steady long-range order magnetic interactions at room-temperature since pristine graphene and TMDs are not spin-polarized and are hard to substitutionally dope by transition metals[7]. It has been confirmed in latest studies that nanoscale materials comprising of transition metals (TMs) with open d-orbital shells could reveal a multitude of stimulating properties due to diverse oxidation and spin states, and comparatively greater spin-orbit coupling of the TMs. Therefore, TM-based low-dimensional materials offer an outstanding ground for discovering and developing the internal degrees of freedom of electrons − charge, orbital, and spin − and their relationship for fundamental investigation and device applications [8] [9] [10] [11] . There are various TMs based low-dimensional materials, e.g. dichalcogenides, which may have been potentially exfoliated in experimentation [12] [13]. Amongst them, currently, MXenes are actually at the cutting edge of nanotechnology research and have capacity for novel scientific and industrial perspectives [7] .

These MXenes, a newly discovered group that belongs to 2D materials, include transition metal carbides, carbo-nitrides and nitrides. The general formula for MXene is $M_{n+1}X_nT_x$ (where, M= Sc, Ti, V, Cr, Zr, Nb, Mo, Hf, Ta and X= C, N while n = 1,2,3); the first letter M represents early transition metal, X represents nitrogen or carbon, Tx shows the surface terminations that can be oxygen (O), hydroxyl (OH) or fluorine (F). The most studied compound among MXenes is $Ti_3C_2T_x$

. These advanced 2D nanosheets are termed MXenes because they initiate from the MAX phases by eliminating "A" elements and because they are structurally related to graphene [19]. The $Ti_3C_2T_x$ based MXenes are formed by extracting the aluminium from MAX phase Ti_3AlC_2[14 15 16 17]. To date, more than 60 MAX phases have been discovered, and many of them have been successfully processed into 2D MXene nanosheets. These MXene layered structures are fundamentally predicted theoretically to be ferromagnetic in nature without any electronic band structure or structural variations and hence, can potentially be fabricated in well crystalline form. Another encouraging point of view regarding spintronics applications of MXenes is their predictable Curie temperature which is predicted to be well above the room-temperature[20].

Various experimental reports of $M_{n+1}X_nT_x$ have been presented for different applications such as transparent conductors[21 22], field effect transistors[23], supercapacitors [24 25 26], Li-ion batteries[19 27], electromagnetic interface shielders [28], fillers in polymeric composites [29], hybrid nanocomposites[30], purifiers[31 32], dual-responsive surfaces[33], suitable substrates for dyes [34], catalysts [35 36], promising materials for methane storage[37], and photocatalysts for hydrogen production[38], as well as being ceramic biomaterials with high photothermal conversion efficiency for cancer therapy[39]. Computationally, many applications have been proposed for MXenes in electronic[40 41 42 43 44], magnetic[45 46 47 48 49], optical[50 51], thermoelectric[48 52 53 54 55 56], and sensing devices [57], as well as being new potential materials for catalytic and photocatalytic reactions[18 58 59 60 61 62], hydrogen storage media[63 64], and nanoscale superconductivity[65]. Some of the MXenes are predicted to be topological insulators with large band gaps involving only d-orbitals [66 67 68 69]. The $M_{n+1}X_nT_x$ nanosheets are also expected to be used as ultralow work function materials [70] and Schottky barrier junctions [71 72 73].

The computational and experimental reports given above have proposed that MXenes are attractive 2D structures due to the subsequent motives: (1) due to their ceramic nature, $M_{n+1}X_nT_x$ are structurally and chemically stable, (2) these $M_{n+1}X_nT_x$ can be originated in diverse forms of mono-layer, bi-layer, few-layers and multi-layers, (3) $M_{n+1}X_nT_x$ can be manufactured as multifaceted

system made up of mixture of light and heavy TMs that makes it promising to adjust the number of outer most electrons and the relativistic spin-orbit interactions. This improves their electronic efficiency and mechanical strength, (4) the thickness of $M_{n+1}X_nT_x$ mono-layers is well-behaved and controllable which enable us to inspect the quantum confinement associated phenomena, (5) the surfaces of $M_{n+1}X_nT_x$ can be functionalized with several elemental groups, which suggest opportunities for surface state engineering, (6) comparable to graphene, some of $M_{n+1}X_nT_x$ reveal massless Dirac dispersions in their band structures adjacent to the Fermi level [66 67 68 69 74]. This opens-up broad possibilities to study and explore the Dirac-based physics[66 67 68 69]. These properties mark $M_{n+1}X_nT_x$ exceptional candidate among other recognized 2D systems though few of them have not been experimentally perceived yet.

Consequently, for commercial grade devices, large areas with higher carrier concentration 2D room-temperature ferromagnetic nanoscale materials are desirable. The current work is focused on synthesis of undoped and Gadolinium-doped 2D $Ti_3C_2T_x$ MXene and to study the effect of doping in terms of bandgap, optical properties, and magnetic properties. The present work motivates a new direction for semiconducting 2D materials-based spintronic devices for memory storage applications to be used at room-temperature.

EXPERIMENTAL

For the selective etching of Aluminium (Al) from MAX (here known as Ti_3AlC_2), typically 10 grams of MAX powder was dissolved in 230ml of Hydrofluoric acid (HF, 39 wt%) at room-temperature in closed Teflon bottle under constant magnetic stirring for 66 hours. After the completion of the reaction, the products were washed number of times with ethanol and de-ionized (DI) water in order remove any acidic residues until a pH of 6 was obtained. Followed by vacuum filtration, the powder was dried in a convection oven at 100 ℃ for about 10 hours. The final product was etched MXene (Ti_3C_2) sheets.

In Supplimentary Information (SI), there is simplified reaction occur when Ti_3AlC_2 is immersed in HF. We present indication for these reaction with the surface group F and/or OH, which give results in exfoliated layers of MXene (Ti_3C_2). Hence, it is assumed from reactions SI(2) and SI(3) that terminations are –F or –OH, in fact they are most possibly combination of both. The layers of Ti_3C_2 completely disperse by the Al atoms, which ultimately lead to formation of MAX (Ti_3AlC_2). After reaction SI(1), Al atoms are detached from Ti_3C_2 layers due to which Ti_3C_2 layers are also scraped from each other. The main reason to it is the dropping of metallic bonding which is actually the firm holder of the Ti_3C_2 layers in presence of Al atoms.[15]

The Gadolinium (Gd^{+3}) doped MXene (General formula: $Ti_{3(1-x)}Gd_xC_2(OH)_2$) with the stoichiometric ratio of 1:1 was synthesized by co-precipitation method. Ti_3C_2 solution was prepared in deionized water with a concentration of 0.4mg/ml and was sonicated for 10 minutes at room-temperature. The dopant Gadolinium Nitrate Hexahydrate ($Gd(NO_3)_3.6H_2O$) powder was added to ethylene glycol and acetic acid in a ratio of 1:1, molarity of 0.01 M was used as a solvent and sonicated for 1h at room-temperature. After that, both the separated solutions were mixed together and sonicated for half an hour. After sonication, final solution was put on hot plate for 3h under stirring. The prepared solution was washed with deionized water several times and a homogenous fine powder was obtained, which was put in drying oven at 100°C for 24 h.

Structural diffraction measurements were performed via X-ray diffractometer (XRD) by using monochromatic Cu-Kα radiation wavelength of (λ=1.5405nm) under 40 kV voltage source and 200 mA current with 2θ altering from 5° to 65°. Scanning electron microscopy (SEM) was used to study morphology and particle size of samples. Energy Dispersive Spectrometer (EDS) characterization technique was used to study the chemical ingredients of the samples. The band-gap was calculated by UV-Vis diffused reflectance spectra via UV-Vis spectrophotometer with an integration sphere. Infrared spectra (FTIR) of the samples were measured by using the Fourier-transform (FT-IR) spectrometer. The frequency ranges between 4000-400 cm^{-1} using KBr as diluent.

RESULTS AND DISCUSSIONS:

X-RAY DIFFRACTION

X-ray Diffractometer was used to investigate the crystal structure by powder diffraction patterns of undoped MXene (Ti_3C_2) and Gd-doped MXene (Gd-Ti_3C_2) nanosheets as presented in **Figure 1**. All the diffracted peaks of these nanosheets sample are well matched with hexagonal crystal structure as reported earlier[75] [76]. The diffraction plane (003) at 2θ ~ 28.5° represents the characteristics of TiO_2 peak, in which Gd^{+3} shows a complex structure with Ti^{+4} on surface in the form of oxides[77]. The peak at 2θ ~ 39.2° is very sharp in undoped sample which shows the presence of Al in MXene as it usually retained MAX sheet; after doping the peak is supressed as reported in literature [19]. The peak present at 34.5°, 38.1°, 40.2°, shows a small quantity of Al_2O_3 as nano-crystals which is not removed completely by etching on the surface of MAX to get MXene [78].

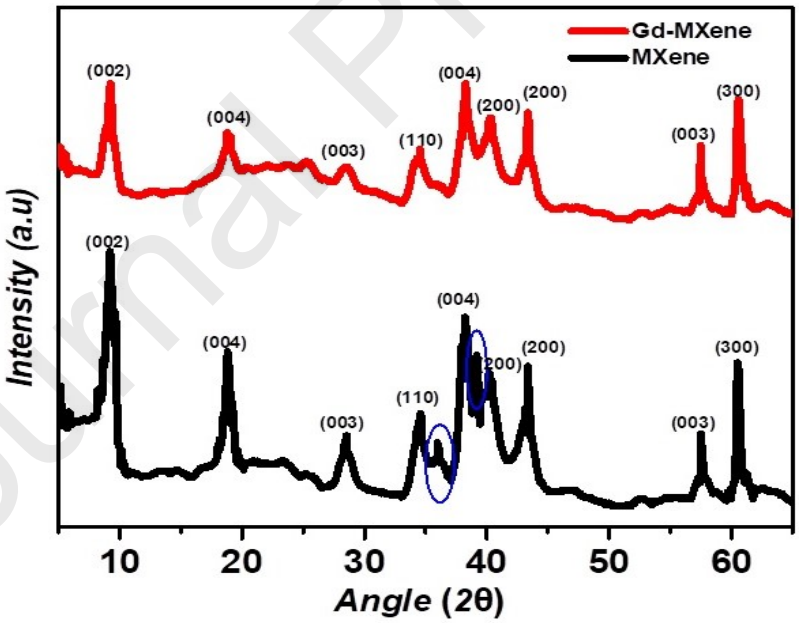

Figure 1: XRD pattern of MXene (Ti_3C_2) and Gd-doped MXene (Gd/Ti_3C_2).

The peak at 2θ ~43° and 2θ~ 60.5° is suppressed and show the characteristics of titanium carbide in crystal structure[79]. We noticed, overall the intensity of Gd-doped sample has been reduced (i.e.

sharpness suppressed) as compared to undoped MXene. While, there is right shift in peak positions observed in doped sample as compared to undoped one. This shifting in higher 2 theta values might be caused by two possible effects; ion-exchange mechanism and strong electrostatic interaction, it also gives aspect that there is no intercalation. During the chemical reaction, positive ions are appeared in access and around MXene sheets which create a strong electrostatic potential that interacts with negatively charged surface and cause the formation of a complex interaction between the negative terminations and positive Gd^{+3} ions. The shifting of peak positions typically caused by this strong electrostatic interaction that makes sure the doping of Gd^{+3} ion species in the crystal structure of MXene. However, due to larger radius of Gd^{+3}, the ability to lose electron is greater and probably Gd^{+3} also creates more positive potential around the surface of MXene. The ionic radii of Gd^{+3} is (0.938 Å) which is much larger than the ionic radii of Ti^{+4} (0.605 Å). Thus, it is very hard for Gd^{+3} ions to substitute into the structure of Ti_3C_2 and replace Ti^{+4} ions, however, no structure change is supposed for Gd^{+3} doped samples, indicating that the doped Gd^{+3} occur at the boundary of crystal rather than into the inner structure of the crystal lattice of Ti_3C_2[80].

The lattice parameters of MXene and Gd-doped MXene nanosheets samples are calculated by equation of plane spacing for Hexagonal crystal structure;[81]

$$\frac{1}{d^2}=\frac{4}{3}\left(\frac{h^2+hk+k^2}{a^2}\right)+\frac{l^2}{c^2}$$

Where, hkl are Miller indices. The lattice parameter a=b=5.3Å and c=19.20Å for undoped MXene and higher order values a=b=5.4Å and c=19.30Å for Gd-doped nanosheets has been measured. By using line broadening analysis of X-ray, the particles crystallite size can be calculated[82]. The Scherrer's formula $D= K\lambda/\beta\cos\theta$ was used to calculate the particle size from broadening the diffraction peak. The particle size for undoped and doped MXene nanosheets are calculated in the range ~19 nm and ~26 nm, respectively.

and Gd-doped MXene.

X	a (Å)	c (Å)	c/a	Crystallite size (nm)
MXene (Ti_3C_2)	**5.3 Å**	**19.2 Å**	**3.622**	**18.9 nm**
Gd-doped Ti_3C_2	**5.4 Å**	**19.3 Å**	**3.574**	**25.6 nm**

MORPHOLOGICAL ANALYSIS

Microstructural measurement was performed for $Ti_3C_2T_x$ and Gd-doped $Ti_3C_2T_x$ nanosheets as shown in **Figure 2**. It is observed that the $Ti_3C_2T_x$ has a perfect layered structure, where the nano-sheets are clearly separated from each other[76 83] as can be seen in **Figure. 2a**. From SEM image for the doped sample shown in **Figure. 2b**, we did not see any attachment or adsorption of Gd ions with layered structures so we may infer that Gd ions has properly doped into the structure of MXene. The Energy Dispersive X-ray (EDX) spectroscopy provides the information about the elemental compositions in nanosheets samples as presented for undoped and Gd-doped MXene sample in **Figure 2(c, d),** respectively. The EDS spectra clearly confirmed the presence of elemental peaks of C, F, Si, O, Ti, and Al in both samples with additional signal of Gd in doped MXene sample. The weight (wt. %) concentration of each element has been represented in **table-1**. The presence of Gd-dopant is confirmed as a weight % (0.59) present in the measured spectra. The presence of Al is also confirmed which means that it is not completely removed even after achieving MXene phase.

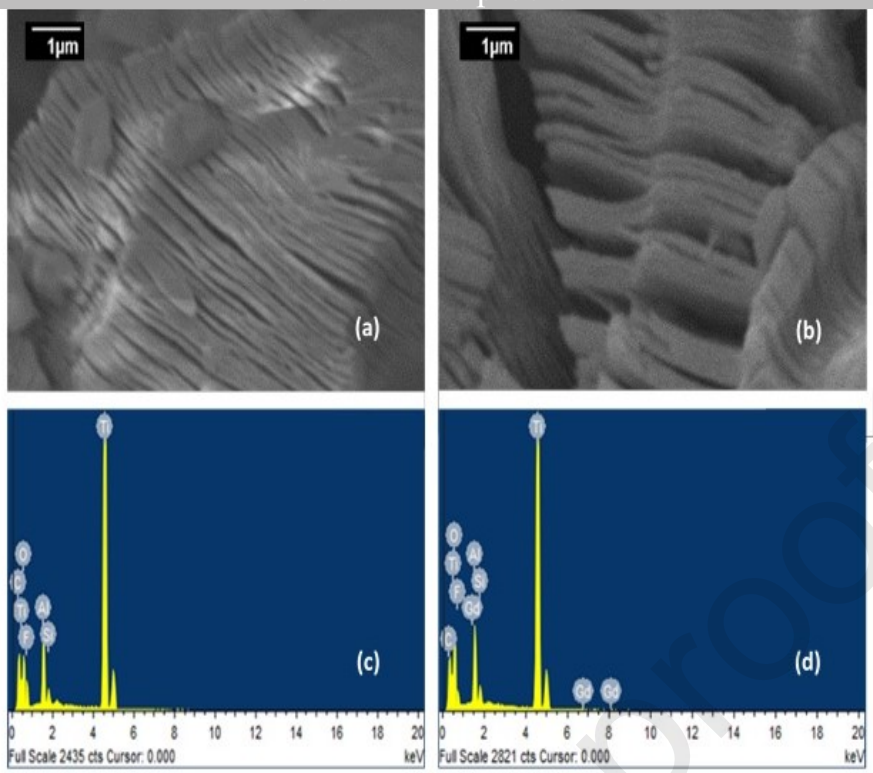

Figure 2: (a,b) SEM micrographs of undoped and Gd-doped MXene **(c)** EDX of undoped MXene **(d)** EDX of Gd-doped MXene.

OPTICAL PROPERTIES

Room-temperature FTIR spectra in the range 400-4000 cm^{-1} for nanosheet samples have been demonstrated in **Figure 3(a)** in determining the extent of oxidation/reduction of materials. A sharp peak at 585 cm^{-1} and 636 cm^{-1} is observed **(inset Figure 3(a))** in spectra of Gd^{+3} doped nanosheet sample that shows that Gd^{+3} combines with Ti-O on the surface and provides a complex structure in the form of oxide [80]. Interestingly, in FTIR absorption, a small hump at position 975 cm^{-1} has been observed in Gd-doped samples as compared to pure MXene as represented in **Figure 3(a).** A small intense peak lies at position 1986 cm^{-1} may due to stretching of C=O and C=C while at 2094 cm^{-1}, a sharp high intense peak represents triple bond C≡C stretching absorption. Thus, this stretching is due to the high force constant of the bond[84]. The peak at 2329 cm^{-1} is usually observed in MXene (Ti_3C_2) nanosheets[85].

Room-temperature optical absorption spectra of both samples are investigated by using a UV-visible spectrophotometer under the wavelength range (200-700 nm) as is shown in **Figure 3(b).** The band gap absorption measurement is calculated using the Kubelka-Munk function[86]. The relation between the absorption coefficient 'α' and the photon energy 'hυ' is given in S1. Wherever, 'A' is ineffective equation constant, 'h' is Plank's constant, "υ" is light frequency, 'E_g' represents band gap energy, respectively[87].

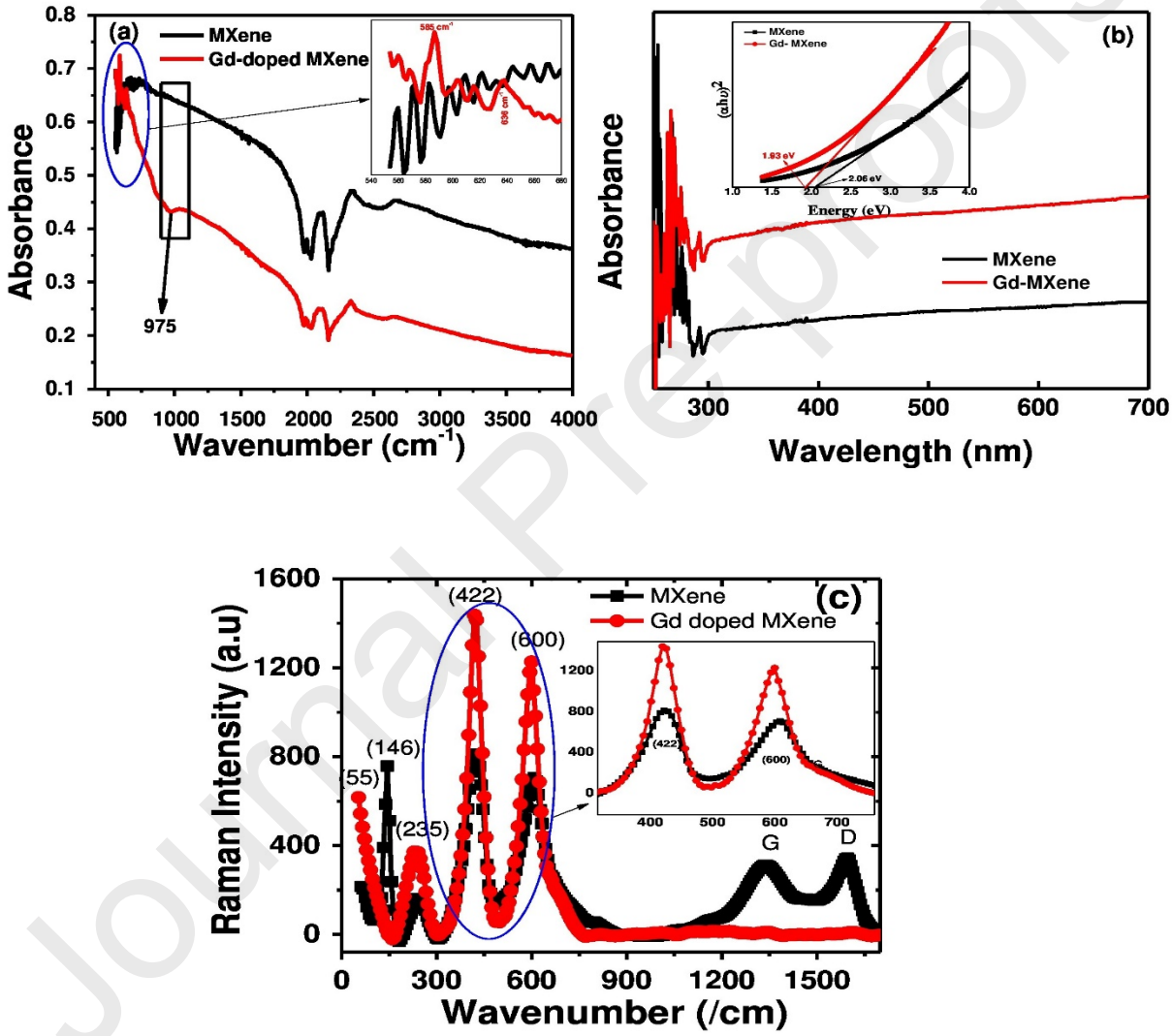

Figure 3: (a) FTIR **(b)** UV-Vis absorption spectra; (inset) bandgap energy **(c)** Room-temperature Raman spectra.

The value of "n" is for the possible absorbance ways to determine the type of transition, n=1 for direct band gap transition and n=4 for the indirect bandgap transition. The band gap of undoped and

Gd-doped MXene sample was obtained by plotting $(\alpha h\upsilon)^2$ against band gap energy Eg also known as Tauc's plot method [91 92] such as presented in inset of **Figure 3(b).** The band gap of MXene is established to be 2.06 eV and the band gap for the Gd-doped MXene is reduced to 1.93 eV. For Gd-doped MXene nanosheets, the red shift is observed in the absorption spectra as compared to pure MXene. In Gd-doped MXene, the slight reduction in the band gap energy has been observed as reported previously [93]. As E_g for Gd-doped MXene is smaller than those for un-doped MXene, it is an indication that new electronic levels (sub-bands) will be introduced by doping ions inside the MXene band-gap as reported earlier for 2-dimensional nanosheets semiconductor systems [86 91 94 95 96]

Raman spectrum of Ti_3C_2 MXenes has several broad peaks ranging from 50 to 1600 cm^{-1}, which can be assigned to non-stoichiometric titanium carbide as shown in **Figure 3(c).** According to the crystallographic structure of Ti_3C_2, the 5 atoms of the primitive unit cell in the Ti_3C_2 nanosheet contribute rise to 12 optical modes and 3 acoustic modes at the Γ point of the Brillouin zone[97]. The optical phonons at the center of the Brillouin zone for Ti_3C_2 are given in SI [97-99]. All Raman vibration modes of Gd-doped sample are shifted toward lower wavenumber as compared to undoped sample as shown inset Figure 3(c). While interestingly, we noticed that the intensity of each mode has enhanced in Gd-doped as compared to undoped sample.

In literature for Ti_3AlC_2, phonon vibration at 150 cm^{-1} was assigned to the Al atoms related vibration modes[100]. The Raman peak lies at 146 cm^{-1} may be due to phonon vibration of Ti_3AlC_2 (MAX) as reported previously [101]. In literature, frequency associated with doubly degenerated E_g modes at 146 cm^{-1} in the bare Ti_3C_2 nanosheet may reflect the main contribution is from in-plane vibrations of Ti_2 and C atoms which may correspond to the anatase crystal structure [23]. In Gd-doped sample, we did not observe mode at 146 cm^{-1}, usually lower-frequency (<500 cm^{-1}) phonons are due to collaborative motion of all atoms in the nanosheets. It is noteworthy that no robust signal of TiO_2 was detected [102] (as we obtained 146 cm^{-1} in pure sample) in Gd-doped MXene sample, indicating that either the $Ti_3C_2T_x$ sheets are not oxidized, or limited MXene flakes are oxidized that is beyond the detection of Raman technique, indicating low density of anatase TiO_2 on the surface of $Ti_3C_2T_x$.

The remaining peaks of the pristine Ti_3C_2 nanosheet sample and Gd-doped MXene belong to Ti−C vibrations. In the Ti_3C_2 nanosheets, the modes assigned at 235 cm^{-1} and 600 cm^{-1} position relates with $A1_g$ group and correspond to out-of-plane stretching vibrations of Ti_2 and C, respectively [97-99]. The vibrational phonon at position 422 cm^{-1} belongs to E_g Raman modes that may be assigned to $Ti_3C_2(OH)_2$ phase existence for in-plane modes vibrations[99] . The two broad peaks between 1350 cm^{-1} and 1580 cm^{-1} belong to the D–band (is associated with disordered graphite structure and defects) and G–band (originates from the signal from graphite) of graphitic carbon [103]. Both G and D peaks are due to sp^2 sites. The G-mode peak is associated with the stretching of the C-C bond in carbon materials and is common to all sp2 carbon systems in both, rings and chains [104]. The D mode peak depends on sp^2 fraction and order and appears only if the sp^2 is in disordered rings. In undoped MXene sample, the presence of carbon sheets (G and D band) covered by TiO_2 (mode 146cm-1) particles on the surface implies that the innermost Ti atoms in the MXene structure migrated outward to react with oxygen. This outward migration of Ti is similar to what has been observed previously during the oxidation of TiN [105]. A different interesting observation in Raman spectra is the absence of D and G bands after Gd-doping in $Ti_3C_2T_x$ nanosheets that might indicate the deformation of carbon [106].

MAGNETIC ANALYSIS

The magnetic hysteresis loops for Gd-doped MXene measured at 300K and 100K are shown in **Figure 4(a, b).** Also, to remove the background signal of the machine that may create its own stray magnetic field that may induce anisotropic magnetic effect, the system was calibrated by using an oscillatory field in order to eliminate the entire stray fields among the coils, so the real magnetic behavior of the sample could be observed. After we were sure of the neutral stray magnetic field, we performed the measurement. The "S-shaped" curve at room temperature with saturation magnetization (Ms) 22×10^{-4}emu/g for undoped MXene **(Fig. S1)** and 80×10^{-4}emu/g for Gd-doped MXene nanosheets at magnetic field of 10 kOe are seen for both samples. At room-temperature, we

noticed the fluctuation in data points of undoped MXene sample as compared to very smooth data points of Gd-doped nanosheets which indicates that undoped sample may require more magnetic fields to stabilize at 300K relative to Gd-doped sample. The measured values of coercivity in kOe (Hc = 0.0887) and remnant magnetization (Mr =0.2298x10^{-4}emu/g) for doped MXene were measured. At the temperature of 100K, the non-saturated hysteresis curve of the undoped and doped samples are shown in **Figures SI and 4(b),** respectively. It can be seen that the saturation magnetization for undoped and doped samples are 3.529x10^{-4} emu/g and 120x10^{-4} emu/g, respectively. These samples showed weak ferromagnetism as demonstrated in Figure SI and Figure 4. The slope of curves at 100K increased as compared to 300K measurements, however another anomaly is found that the Ms value at 100K has been decreased by 5 times for undoped sample as equated to 300K. While, usual behavior has been observed for Gd-doped MXene sample, Ms value increased by factor of almost 42 as measurement temperature decreased from 300K to 100K. This net spin moment interacts more as thermal fluctuation reduces and wave function of unpaired electrons overlaps more vigorously, ultimately saturation magnetization enhances. The increase in saturation magnetization, decrease in coercive fields and increase in remnant magnetization for Gd-doped MXene as compared to undoped MXene might be attributed to the ferromagnetic nature of Gd^{+3} cation which possess excess unpaired spins of electrons and thus, have more net magnetic moment. As a result, the doped MXene shows a good ferromagnetic behavior at room-temperature[107 108 109 110 111 112 113]

It is to be noted that the net magnetic moment for ZFC is lower than for FC due to fact that the magnetic field for FC curves overcome the anisotropic effect of magnetic domains. However, this may also be attributed to the presence of functional groups such as _OH or O-1s which may create an attraction for electron cloud due to its more electronegativity than the Ti and C -cations[48]. It was reported by S. Zhao et al. that the spatial spin-density of states (s-DOS) for spin-up electrons exist at upper layer of Ti-3d cation whereas the s-DOS for spin-down electrons lie at the bottom Ti-3d electrons resulting in an asymmetric net spin moment within the Ti_3C_2 MXene layers[16]. This explains

the presence of low net magnetic moment in undoped MXene. However, it was observed that the doping of Gadolinium cation results in strong magnetic hysteresis loop and large net magnetic moment which indicates that the resultant spatial spin-density of states exceeds more for one type of spin, i.e. spin-up that the other spin. This results in increased magnetic moment for the Gd-doped MXene than for the undoped MXene even for a very small doping concentration.

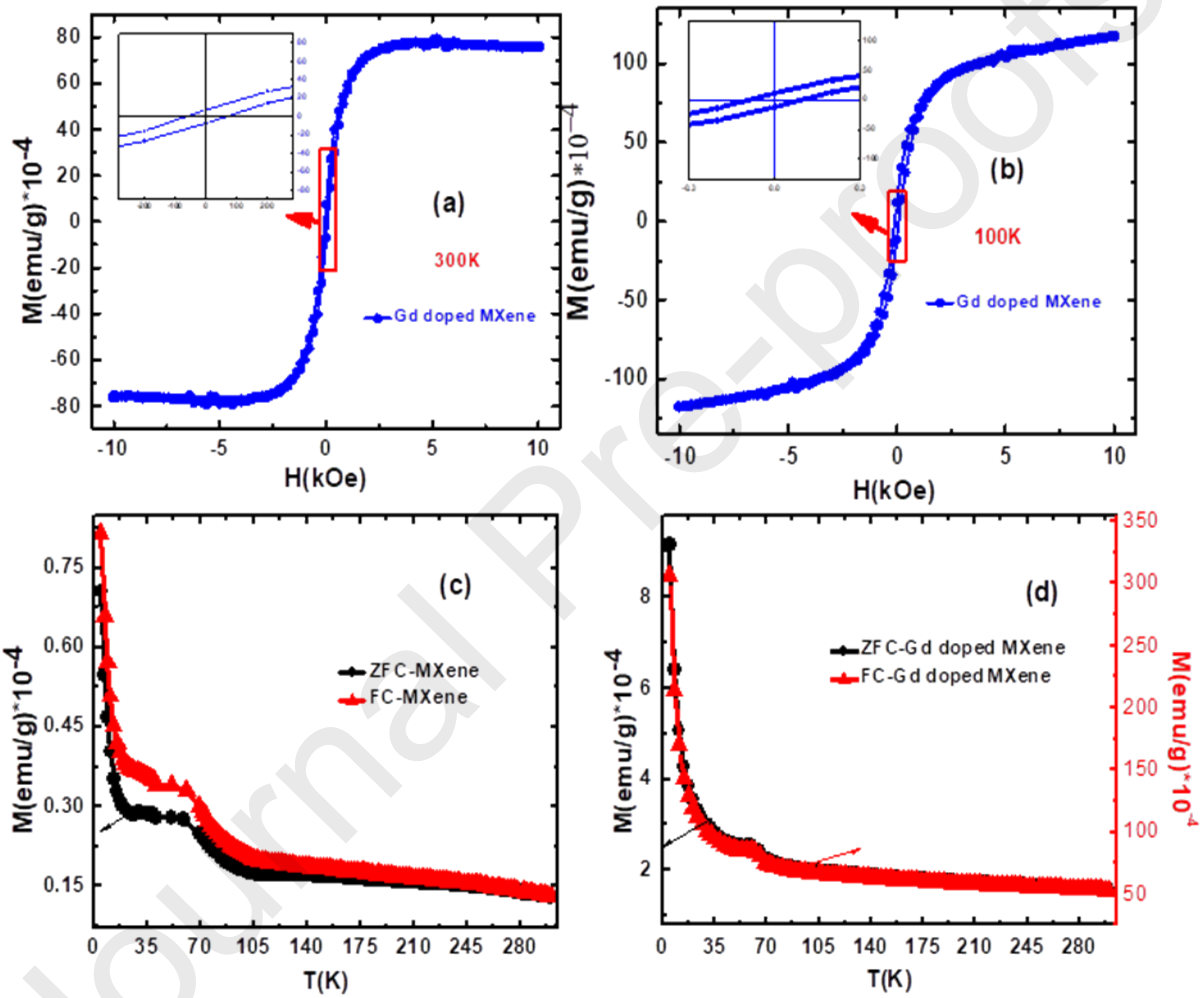

Figure 4: (a) and (b) M-H curves fort Gd-doped MXene at 300K and 100K, respectively, **(c) and (d)** field cool (FC) and zero field cool (ZFC) curves measured at 1000 Oe for undoped MXene and Gd-doped MXene, respectively.

The zero-field cooled (ZFC) and field cooled (FC) temperature measurements known as M(T) of these nanosheets samples were measured at magnetic field strength of 1000 Oe as presented in

Figure 4(c, d) for undoped and Gd-doped samples, respectively. These FC and ZFC curves show the ferro- to para- magnetic phase transition as temperature increased from 5K to 300K. For both samples, the values of FC and ZFC remains well above zero, which is a clear indication of the interaction among unpaired electrons exist and net magnetization will be attained even at room-temperature. From these curves, we noticed that almost FC and ZFC values remains same for undoped MXene while FC values of Gd-doped nanosheets are much higher (e.g. maximum value is $340x10^{-4}$emu/g) than ZFC values (e.g. maximum value is $8.2x10^{-4}$emu/g). We found one discrepancy during M(T) measurements for both samples. We noticed decreasing trend of magnetic moment with increasing temperatures during FC/ZFC measurements however an irregular behavior detected in Figure 4(c, d) for both samples which shows splitting of the FC/ZFC curves at low temperatures. This irregular behavior might be due to the presence of extra impurities (i.e. impurities are present as discussed in the XRD section as TiC and TiO_2). Usually, these impurities are unavoidable due to the nature of chemical synthesis route followed as well as the etching process to get MXene itself from the parent MAX phases.

These observations may suggest that the undoped MXene need more field strength as compared to Gd-doped nanosheets to well align its all unpaired domain in the direction of applied field. The M(T) curves also indicate there is an increase in magnitude and stability of Gd-doped MXene compared to the undoped MXene which makes it a suitable candidate for spintronics applications based on two-dimensional materials.

Figure 5 summarizes the overall synthesis and reasoning for origin of ferromagnetism in Gd-doped MXene at room-temperature.

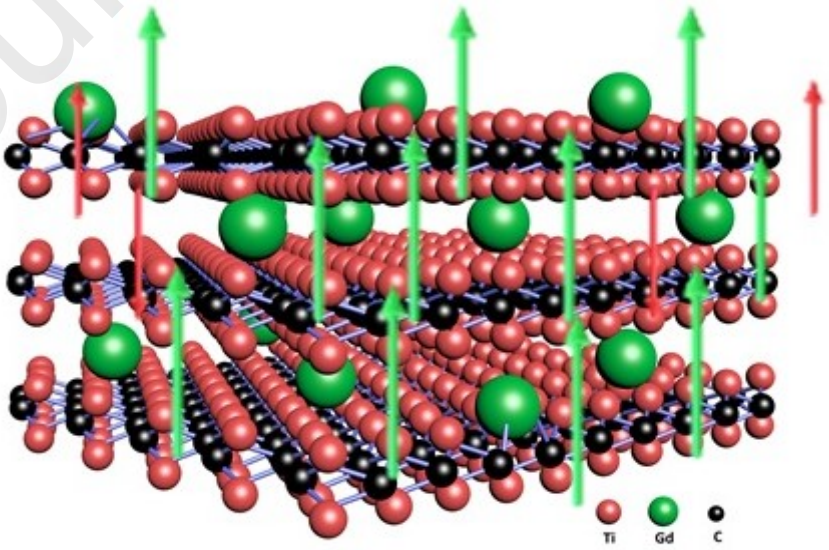

Figure 5: A schematic illustration of Gd-doped MXene with enhanced magnetic properties.

CONCLUSION

The 2D undoped and Gd-doped Ti_3C_2-MXene sheets were prepared using co-precipitation method. The structural, morphological, elemental and bandgap characterizations showed the successful doping of Gadolinium into the MXene sheets. The Gd-doped MXene indicate its semi-conductive nature. The magnetic measurement showed that the Gd-doped sample possess a high magnetic moment at room-temperature with a stable ferromagnetic hysteresis loop. The origin of magnetism lies in the fact that the electrons in Ti-3d has measurable spin-density of states around Fermi level which enhances upon doping of ferromagnetic Gadolinium cation, making it a perfect soft ferromagnet. The successful doping, reduction of the band-gap and introduction of strong ferromagnetic signal at room-temperature makes our sample a suitable candidate for spintronic devices and opens up more scope for the rare-earth elements doping into MXene sheets.

ACKNOWLEDGMENT

The authors are thankful to Higher Education Commission (HEC) of Pakistan for providing research funding under the Project No.: 6040/Federal/NRPU/R&D/HEC/2016 and HEC/USAID for financial support under the Project No.: HEC/R&D/PAKUS/2017/783. The author also thanks School of Natural Sciences (SNS) at National University of Science & Technology (NUST), Islamabad, Pakistan for partial financial support.

REFERENCES

1 Young-Woo Son, Marvin L Cohen, and Steven G Louie, Nature **444** (7117), 347 (2006).

2 Yan Wang, Yi Huang, You Song, Xiaoyan Zhang, Yanfeng Ma, Jiajie Liang, and Yongsheng Chen, Nano letters **9** (1), 220 (2008).

3 Kathleen M McCreary, Adrian G Swartz, Wei Han, Jaroslav Fabian, and Roland K Kawakami, Physical review letters **109** (18), 186604 (2012).

N Levy, SA Burke, KL Meaker, M Panlasigui, A Zettl, F Guinea, AH Castro Neto, and MF Crommie, Science **329** (5991), 544 (2010).

5 RR Nair, M Sepioni, I-Ling Tsai, O Lehtinen, J Keinonen, AV Krasheninnikov, T Thomson, AK Geim, and IV Grigorieva, Nature Physics **8** (3), 199 (2012).

6 Sefaattin Tongay, Sima S Varnoosfaderani, Bill R Appleton, Junqiao Wu, and Arthur F Hebard, Applied Physics Letters **101** (12), 123105 (2012).

7 Ivana Vobornik, Unnikrishnan Manju, Jun Fujii, Francesco Borgatti, Piero Torelli, Damjan Krizmancic, Yew San Hor, Robert J Cava, and Giancarlo Panaccione, Nano letters **11** (10), 4079 (2011).

8 Qing Hua Wang, Kourosh Kalantar-Zadeh, Andras Kis, Jonathan N Coleman, and Michael S Strano, Nature nanotechnology **7** (11), 699 (2012).

9 Sheneve Z Butler, Shawna M Hollen, Linyou Cao, Yi Cui, Jay A Gupta, Humberto R Gutiérrez, Tony F Heinz, Seung Sae Hong, Jiaxing Huang, and Ariel F Ismach, ACS nano **7** (4), 2898 (2013).

10 Gianluca Fiori, Francesco Bonaccorso, Giuseppe Iannaccone, Tomás Palacios, Daniel Neumaier, Alan Seabaugh, Sanjay K Banerjee, and Luigi Colombo, Nature nanotechnology **9** (10), 768 (2014).

11 Ganesh R Bhimanapati, Zhong Lin, Vincent Meunier, Yeonwoong Jung, Judy Cha, Saptarshi Das, Di Xiao, Youngwoo Son, Michael S Strano, and Valentino R Cooper, ACS nano **9** (12), 11509 (2015).

12 JN Coleman, M Lotya, A O'Neill, SD Bergin, PJ King, U Khan, K Young, and A Gaucher, Stanton, HY Kim, K. Lee, GT Kim, GS Duesberg, T. Hallam, JJ Boland, JJ Wang, JF Donegan, JC Grunlan, G. Moriarty, A. Shmeliov, RJ Nicholls, JM Perkins, EM Grieveson, K. Theuwissen, DW McComb, PD Nellist and V. Nicolosi, Science **331** (6017), 568 (2011).

13 Hua Zhang, ACS nano **9** (10), 9451 (2015).

14 Babak Anasori, Maria R Lukatskaya, and Yury Gogotsi, Nature Reviews Materials **2** (2), 16098 (2017).

15 Michael Naguib, Murat Kurtoglu, Volker Presser, Jun Lu, Junjie Niu, Min Heon, Lars Hultman, Yury Gogotsi, and Michel W Barsoum, Advanced Materials **23** (37), 4248 (2011).

16 IR Shein and AL Ivanovskii, Computational Materials Science **65**, 104 (2012).

17 Babak Anasori, Yu Xie, Majid Beidaghi, Jun Lu, Brian C Hosler, Lars Hultman, Paul RC Kent, Yury Gogotsi, and Michel W Barsoum, ACS nano **9** (10), 9507 (2015).

18 M Abdullah Iqbal, S Irfan Ali, Faheem Amin, Ayesha Tariq, Muhammad Z Iqbal, and Syed Rizwan, ACS Omega **4** (5), 8661 (2019).

19 Michael Naguib, Joseph Halim, Jun Lu, Kevin M Cook, Lars Hultman, Yury Gogotsi, and Michel W Barsoum, Journal of the American Chemical Society **135** (43), 15966 (2013).

Liang Dong, Hemant Kumar, Babak Anasori, Yury Gogotsi, and Vivek B Shenoy, The journal of physical chemistry letters **8** (2), 422 (2017).

[21] Joseph Halim, Maria R Lukatskaya, Kevin M Cook, Jun Lu, Cole R Smith, Lars-Åke Näslund, Steven J May, Lars Hultman, Yury Gogotsi, and Per Eklund, Chemistry of Materials **26** (7), 2374 (2014).

[22] Marina Mariano, Olha Mashtalir, Francisco Q Antonio, Won-Hee Ryu, Bingchen Deng, Fengnian Xia, Yury Gogotsi, and André D Taylor, Nanoscale **8** (36), 16371 (2016).

[23] Yajie Yang, Sima Umrao, Shen Lai, and Sungjoo Lee, The journal of physical chemistry letters **8** (4), 859 (2017).

[24] Shen Lai, Jaeho Jeon, Sung Kyu Jang, Jiao Xu, Young Jin Choi, Jin-Hong Park, Euyheon Hwang, and Sungjoo Lee, Nanoscale **7** (46), 19390 (2015).

[25] Maria R Lukatskaya, Olha Mashtalir, Chang E Ren, Yohan Dall'Agnese, Patrick Rozier, Pierre Louis Taberna, Michael Naguib, Patrice Simon, Michel W Barsoum, and Yury Gogotsi, Science **341** (6153), 1502 (2013).

[26] Michael Ghidiu, Maria R Lukatskaya, Meng-Qiang Zhao, Yury Gogotsi, and Michel W Barsoum, Nature **516** (7529), 78 (2014).

[27] Raghavan B Rakhi, Bilal Ahmed, Mohamed N Hedhili, Dalaver H Anjum, and Husam N Alshareef, Chemistry of Materials **27** (15), 5314 (2015).

[28] Yu Xie, Yohan Dall'Agnese, Michael Naguib, Yury Gogotsi, Michel W Barsoum, Houlong L Zhuang, and Paul RC Kent, ACS nano **8** (9), 9606 (2014).

[29] Faisal Shahzad, Mohamed Alhabeb, Christine B Hatter, Babak Anasori, Soon Man Hong, Chong Min Koo, and Yury Gogotsi, Science **353** (6304), 1137 (2016).

[30] Xiaodong Zhang, Jianguang Xu, Hui Wang, Jiajia Zhang, Hanbing Yan, Bicai Pan, Jingfang Zhou, and Yi Xie, Angewandte Chemie International Edition **52** (16), 4361 (2013).

[31] Maoquan Xue, Zhiping Wang, Feng Yuan, Xianghua Zhang, Wei Wei, Hua Tang, and Changsheng Li, RSC Advances **7** (8), 4312 (2017).

[32] Qiuming Peng, Jianxin Guo, Qingrui Zhang, Jianyong Xiang, Baozhong Liu, Aiguo Zhou, Riping Liu, and Yongjun Tian, Journal of the American Chemical Society **136** (11), 4113 (2014).

[33] Jianxin Guo, Qiuming Peng, Hui Fu, Guodong Zou, and Qingrui Zhang, The Journal of Physical Chemistry C **119** (36), 20923 (2015).

[34] Jing Chen, Ke Chen, Dingyi Tong, Youju Huang, Jiawei Zhang, Jianming Xue, Qing Huang, and Tao Chen, Chemical Communications **51** (2), 314 (2015).

[35] Olha Mashtalir, Kevin M Cook, VN Mochalin, M Crowe, Michel W Barsoum, and Y Gogotsi, Journal of Materials Chemistry A **2** (35), 14334 (2014).

Guangyin Pan, Xiaojing Li, Yuling Ma, Yun Zhang, Jiangtao Wu, Bin Xu, Ying Sun, Daojiang Gao, and Jian Bi, New Journal of Chemistry **41** (7), 2793 (2017).

[37] Zhi Wei Seh, Kurt D Fredrickson, Babak Anasori, Jakob Kibsgaard, Alaina L Strickler, Maria R Lukatskaya, Yury Gogotsi, Thomas F Jaramillo, and Aleksandra Vojvodic, ACS Energy Letters **1** (3), 589 (2016).

[38] Fanfan Liu, Aiguo Zhou, Jinfeng Chen, Heng Zhang, Jianliang Cao, Libo Wang, and Qianku Hu, Adsorption **22** (7), 915 (2016).

[39] Jingrun Ran, Guoping Gao, Fa-Tang Li, Tian-Yi Ma, Aijun Du, and Shi-Zhang Qiao, Nature communications **8**, 13907 (2017).

[40] Han Lin, Xingang Wang, Luodan Yu, Yu Chen, and Jianlin Shi, Nano letters **17** (1), 384 (2016).

[41] Mohammad Khazaei, Masao Arai, Taizo Sasaki, Chan-Yeup Chung, Natarajan S Venkataramanan, Mehdi Estili, Yoshio Sakka, and Yoshiyuki Kawazoe, Advanced Functional Materials **23** (17), 2185 (2013).

[42] Andrey N Enyashin and Alexander L Ivanovskii, The Journal of Physical Chemistry C **117** (26), 13637 (2013).

[43] Yu Xie and PRC Kent, Physical Review B **87** (23), 235441 (2013).

[44] Mohammad Khazaei, Ahmad Ranjbar, Mahdi Ghorbani-Asl, Masao Arai, Taizo Sasaki, Yunye Liang, and Seiji Yunoki, Physical Review B **93** (20), 205125 (2016).

[45] Li Feng, Xian-Hu Zha, Kan Luo, Qing Huang, Jian He, Yijun Liu, Wei Deng, and Shiyu Du, Journal of Electronic Materials **46** (4), 2460 (2017).

[46] Chen Si, Jian Zhou, and Zhimei Sun, ACS applied materials & interfaces **7** (31), 17510 (2015).

[47] Junjie He, Pengbo Lyu, LZ Sun, Angel Morales Garcia, and Petr Nachtigall, Journal of Materials Chemistry C **4** (27), 6500 (2016).

[48] Mohammad Khazaei, Ahmad Ranjbar, Masao Arai, Taizo Sasaki, and Seiji Yunoki, Journal of Materials Chemistry C **5** (10), 2488 (2017).

[49] Guoying Gao, Guangqian Ding, Jie Li, Kailun Yao, Menghao Wu, and Meichun Qian, Nanoscale **8** (16), 8986 (2016).

[50] Jianhui Yang, Xuepiao Luo, Shaozheng Zhang, and Liang Chen, Physical Chemistry Chemical Physics **18** (18), 12914 (2016).

[51] H Lashgari, MR Abolhassani, A Boochani, SM Elahi, and J Khodadadi, Solid State Communications **195**, 61 (2014).

[52] Mohammad Khazaei, Masao Arai, Taizo Sasaki, Mehdi Estili, and Yoshio Sakka, Physical Chemistry Chemical Physics **16** (17), 7841 (2014).

Appala Naidu Gandi, Husain N Alshareef, and Udo Schwingenschlögl, Chemistry of Materials **28** (6), 1647 (2016).

[54] S Kumar and Udo Schwingenschlögl, Physical Review B **94** (3), 035405 (2016).

[55] Xian-Hu Zha, Jie Zhou, Yuhong Zhou, Qing Huang, Jian He, Joseph S Francisco, Kan Luo, and Shiyu Du, Nanoscale **8** (11), 6110 (2016).

[56] Xian-Hu Zha, Qing Huang, Jian He, Heming He, Junyi Zhai, Joseph S Francisco, and Shiyu Du, Scientific reports **6**, 27971 (2016).

[57] Xian-Hu Zha, Jingshuo Yin, Yuhong Zhou, Qing Huang, Kan Luo, Jiajian Lang, Joseph S Francisco, Jian He, and Shiyu Du, The Journal of Physical Chemistry C **120** (28), 15082 (2016).

[58] Xue-fang Yu, Yan-chun Li, Jian-bo Cheng, Zhen-bo Liu, Qing-zhong Li, Wen-zuo Li, Xin Yang, and Bo Xiao, ACS applied materials & interfaces **7** (24), 13707 (2015).

[59] Ayesha Tariq, S Irfan Ali, Deji Akinwande, and Syed Rizwan, ACS Omega **3** (10), 13828 (2018).

[60] Chongyi Ling, Li Shi, Yixin Ouyang, and Jinlan Wang, Chemistry of Materials **28** (24), 9026 (2016).

[61] Yuanju Qu, Mengmeng Shao, Yangfan Shao, Mingyang Yang, Jincheng Xu, Chi Tat Kwok, Xingqiang Shi, Zhouguang Lu, and Hui Pan, Journal of Materials Chemistry A **5** (29), 15080 (2017).

[62] Zhonglu Guo, Jian Zhou, Linggang Zhu, and Zhimei Sun, Journal of Materials Chemistry A **4** (29), 11446 (2016).

[63] Haijun Zhang, Guang Yang, Xueqin Zuo, Huaibao Tang, Qun Yang, and Guang Li, Journal of Materials Chemistry A **4** (33), 12913 (2016).

[64] Qianku Hu, Dandan Sun, Qinghua Wu, Haiyan Wang, Libo Wang, Baozhong Liu, Aiguo Zhou, and Julong He, The Journal of Physical Chemistry A **117** (51), 14253 (2013).

[65] Qianku Hu, Haiyan Wang, Qinghua Wu, Xiaotao Ye, Aiguo Zhou, Dandan Sun, Libo Wang, Baozhong Liu, and Julong He, International Journal of Hydrogen Energy **39** (20), 10606 (2014).

[66] Jun-Jie Zhang and Shuai Dong, The Journal of chemical physics **146** (3), 034705 (2017).

[67] Hongming Weng, Ahmad Ranjbar, Yunye Liang, Zhida Song, Mohammad Khazaei, Seiji Yunoki, Masao Arai, Yoshiyuki Kawazoe, Zhong Fang, and Xi Dai, Physical Review B **92** (7), 075436 (2015).

[68] Mohammad Khazaei, Ahmad Ranjbar, Masao Arai, and Seiji Yunoki, Physical Review B **94** (12), 125152 (2016).

[69] Peng-Fei Liu, Liujiang Zhou, Sergei Tretiak, and Li-Ming Wu, Journal of Materials Chemistry C **5** (35), 9181 (2017).

Chemistry C **4** (48), 11524 (2016).

[71] Mohammad Khazaei, Masao Arai, Taizo Sasaki, Ahmad Ranjbar, Yunye Liang, and Seiji Yunoki, Physical Review B **92** (7), 075411 (2015).

[72] Li-Yong Gan, Yu-Jun Zhao, Dan Huang, and Udo Schwingenschlögl, Physical Review B **87** (24), 245307 (2013).

[73] Hui Zhao, Changwen Zhang, Shengshi Li, Weixiao Ji, and Peiji Wang, Journal of Applied Physics **117** (8), 085306 (2015).

[74] Yuanyue Liu, Hai Xiao, and William A Goddard III, Journal of the American Chemical Society **138** (49), 15853 (2016).

[75] Olha Mashtalir, *Chemistry of two-dimensional transition metal carbides (MXenes)*. (Drexel University, 2015).

[76] Yi Tang, JianFeng Zhu, ChenHui Yang, and Fen Wang, Journal of Alloys and Compounds **685**, 194 (2016).

[77] Jingjing Xu, Yanhui Ao, Degang Fu, and Chunwei Yuan, Colloids and Surfaces A: Physicochemical and Engineering Aspects **334** (1-3), 107 (2009).

[78] LL Wang, YW Sun, YZ Gao, and DM Guo, Surface Engineering **32** (2), 85 (2016).

[79] Michael Naguib Abdelmalak, *MXenes: A New Family of Two-Dimensional Materials and its Application as Electrodes for Li-ion Batteries*. (Drexel University, 2014).

[80] An-Wu Xu, Yuan Gao, and Han-Qin Liu, Journal of Catalysis **207** (2), 151 (2002).

[81] Bernard Dennis Cullity, *Answers to Problems: Elements of X-Ray Diffraction*. (Addison-Wesley Publishing Company, 1978).

[82] Roya Aghababazadeh, Ali Reza Mirhabibi, Jalil Pourasad, Andrew Brown, Rik Brydson, Sara Banijamali, and Neda Ameri Mahabad, Surface science **601** (13), 2864 (2007).

[83] Lisa M Viculis, Julia J Mack, Oren M Mayer, H Thomas Hahn, and Richard B Kaner, Journal of Materials Chemistry **15** (9), 974 (2005).

[84] B Suart, Google Scholar (2004).

[85] Jianmin Luo, Xinyong Tao, Jun Zhang, Yang Xia, Hui Huang, Liyuan Zhang, Yongping Gan, Chu Liang, and Wenkui Zhang, Acs Nano **10** (2), 2491 (2016).

[86] Paul Kubelka, Zeitschrift fur technische Physik **12**, 593 (1931).

[87] Zhinan Ma, Zhenpeng Hu, Xudong Zhao, Qing Tang, Dihua Wu, Zhen Zhou, and Lixin Zhang, The Journal of Physical Chemistry C **118** (10), 5593 (2014).

[88] Guodong Zou, Baozhong Liu, Jianxin Guo, Qingrui Zhang, Carlos Fernandez, and Qiuming Peng, ACS applied materials & interfaces **9** (8), 7611 (2017).

Zhiwei Zhang, Haiming Li, Guodong Zou, Carlos Fernandez, Baozhong Liu, Qingrui Zhang, Jie Hu, and Qiuming Peng, ACS Sustainable Chemistry & Engineering **4** (12), 6763 (2016).

[90] S Myhra, JAA Crossley, and MW Barsoum, Journal of Physics and Chemistry of Solids **62** (4), 811 (2001).

[91] Xiang Xu, Yuan-Hua Lin, Pai Li, Li Shu, and Ce-Wen Nan, Journal of the American Ceramic Society **94** (8), 2296 (2011).

[92] MA Butler, Journal of Applied Physics **48** (5), 1914 (1977).

[93] Syed Irfan, Syed Rizwan, Yang Shen, Liangliang Li, Sajid Butt, and Ce-Wen Nan, Scientific reports **7**, 42493 (2017).

[94] Feng Gao, XY Chen, KB Yin, Shuai Dong, ZF Ren, Fang Yuan, Tao Yu, ZG Zou, and J-M Liu, Advanced Materials **19** (19), 2889 (2007).

[95] Xu Peng, Lele Peng, Changzheng Wu, and Yi Xie, Chemical Society Reviews **43** (10), 3303 (2014).

[96] Yupeng Gao, Libo Wang, Aiguo Zhou, Zhengyang Li, Jingkuo Chen, Hari Bala, Qianku Hu, and Xinxin Cao, Materials Letters **150**, 62 (2015).

[97] Tao Hu, Minmin Hu, Zhaojin Li, Hui Zhang, Chao Zhang, Jiemin Wang, and Xiaohui Wang, The Journal of Physical Chemistry A **119** (52), 12977 (2015).

[98] Tao Hu, Jiemin Wang, Hui Zhang, Zhaojin Li, Minmin Hu, and Xiaohui Wang, Physical Chemistry Chemical Physics **17** (15), 9997 (2015).

[99] Luxi Zhang, Weitao Su, Yanwei Huang, He Li, Li Fu, Kaixin Song, Xiwei Huang, Jinhong Yu, and Cheng-Te Lin, Nanoscale research letters **13** (1), 343 (2018).

[100] Xu Chen, Xueke Sun, Wen Xu, Gencai Pan, Donglei Zhou, Jinyang Zhu, He Wang, Xue Bai, Biao Dong, and Hongwei Song, Nanoscale **10** (3), 1111 (2018).

[101] Bilal Ahmed, Dalaver H Anjum, Mohamed N Hedhili, Yury Gogotsi, and Husam N Alshareef, Nanoscale **8** (14), 7580 (2016).

[102] Xin Guo, Xiuqiang Xie, Sinho Choi, Yufei Zhao, Hao Liu, Chengyin Wang, Song Chang, and Guoxiu Wang, Journal of Materials Chemistry A **5** (24), 12445 (2017).

[103] Sharona A Melchior, Kumar Raju, Innocent S Ike, Rudolph M Erasmus, Guy Kabongo, Iakovos Sigalas, Sunny E Iyuke, and Kenneth I Ozoemena, Journal of The Electrochemical Society **165** (3), A501 (2018).

[104] Roghayyeh Lotfi, Michael Naguib, Dundar E Yilmaz, Jagjit Nanda, and Adri CT Van Duin, Journal of Materials Chemistry A **6** (26), 12733 (2018).

[105] Michael Naguib, Olha Mashtalir, Maria R Lukatskaya, Boris Dyatkin, Chuanfang Zhang, Volker Presser, Yury Gogotsi, and Michel W Barsoum, Chemical communications **50** (56), 7420 (2014).

Xinliang Li, Xiaowei Yin, Meikang Han, Changqing Song, Hanlong Xu, Zexin Hou, Litong Zhang, and Laifei Cheng, Journal of Materials Chemistry C **5** (16), 4068 (2017).

107 TP Bertelli, EC Passamani, C Larica, VP Nascimento, AY Takeuchi, and MS Pessoa, Journal of Applied Physics **117** (20), 203904 (2015).

108 D Errandonea, R Boehler, B Schwager, and M Mezouar, Physical Review B **75** (1), 014103 (2007).

109 N Kamali Sarvestani, A Yazdani, and SA Ketabi, Physical Chemistry Chemical Physics **16** (45), 25191 (2014).

110 ZP Yin and WE Pickett, Physical Review B **74** (20), 205106 (2006).

111 Daniel Errandonea, Reinhard Boehler, and Marvin Ross, Physical review letters **85** (16), 3444 (2000).

112 G Fabbris, T Matsuoka, J Lim, JRL Mardegan, K Shimizu, D Haskel, and JS Schilling, Physical Review B **88** (24), 245103 (2013).

113 Lun Xiong, Jing Liu, Ligang Bai, Xiaodong Li, Chuanlong Lin, and Jung-Fu Lin, Journal of Applied Physics **116** (24), 243503 (2014).

Highlights:

1. This is the first report on rare-earth Gadolinium cation (Gd^{+3}) doping in two-dimensional Ti_3C_2-MXene.

2. The bandgap of the MXene decreased from 2.06eV to 1.93eV after the successful doping of Gd cation. The undoped Ti_3C_2-MXene showed weak signature of ferromagnetism at low-temperature and room-temperature however, the magnetic moment was low and not stable at room-temperature.

3. This experimental evidence gives evidence of ferromagnetism in 2D MXene suitable for 2D spintronics.